THE JOURNAL OF PHYSICAL CHEMISTRY C LETTERS

2007, *111,* 14031−14034
Published on Web 08/31/2007

Temperature Coefficients of Raman Frequency of Individual Single-Walled Carbon Nanotubes

Yingying Zhang, Liming Xie, Jin Zhang,* Zhongyun Wu, and Zhongfan Liu*

Center for Nanoscale Science and Technology (CNST), Beijing National Laboratory for Molecular Sciences (BNLMS), State Key Laboratory for Structural Chemistry of Unstable and Stable Species, and Key Laboratory for the Physics and Chemistry of Nanodevices, College of Chemistry and Molecular Engineering, Peking University, Beijing 100871, P. R. China

Received: June 28, 2007; In Final Form: August 20, 2007

In the present study, individual suspended single-walled carbon nanotubes (SWNTs) were prepared and the temperature coefficients of Raman frequency of 13 SWNTs were measured. It is found that the temperature coefficients of the G-band frequency ($\alpha_{\omega G}$) are similar, around $(-1.67 \pm 0.20)\times10^{-5}$/K, whereas in the case of the radial breathing mode (RBM), the coefficients ($\alpha_{\omega RBM}$) are varied from a minimum value of -1.06×10^{-6}/K to a maximum of -2.30×10^{-4}/K. Larger-diameter nanotubes tend to have larger $\alpha_{\omega RBM}$ values; moreover, nanotubes with similar diameters may show different $\alpha_{\omega RBM}$ values. These results reveal that the $\alpha_{\omega RBM}$ value of individual SWNTs depends on both diameter and chirality.

Resonance Raman spectroscopy (RRS) has been demonstrated to be an effective and nondestructive technique to characterize the structures and electronic properties of single-walled carbon nanotubes (SWNTs).[1] Because the Raman scattering process involves complicated electron−phonon interactions, the study of the temperature effects on the Raman spectra could provide important insight into the physical properties of this unique one-dimensional system.[2] The radial breathing mode (RBM) is a unique feature in the Raman spectra of SWNTs. It involves the collective vibrational movement of carbon atoms toward and away from the central axis of a SWNT.[3] The frequency of RBM (ω_{RBM}) tightly depends on the diameter (d_t) of the SWNT, and the chiral angle (θ) also has some influence on the ω_{RBM} value although the effect is relatively weak.[4] Therefore, it is an interesting and important issue to investigate whether and how the temperature behaviors of ω_{RBM} depend on the d_t and θ values of SWNTs. Currently, because most of the works focused on the temperature dependence of the Raman spectra of SWNTs[2,3,5,6] are done on bulk SWNT samples, in which nanotubes with different d_t and θ values are present, the results could not reveal the relationship between the temperature behavior of ω_{RBM} and the structure of the nanotube. Moreover, it has been proven that the surrounding environments of nanotubes may have a remarkable influence on the properties of nanotubes.[7,8] So individual suspended SWNTs,[9] being free from environmental influence, are an ideal choice for such a study.

Herein, suspended SWNTs were prepared and the temperature coefficients of the Raman frequency of 13 individual SWNTs were measured. While the temperature coefficients of ω_G (frequency of G-band, tangential stretching mode) of different SWNTs demonstrate similar values, the coefficients of ω_{RBM} show an interesting dependence on the structure of the SWNTs.

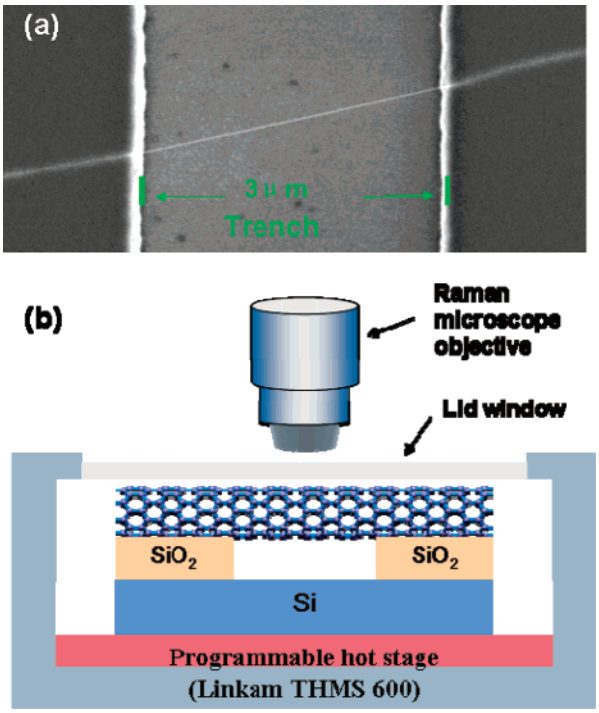

Figure 1. (a) SEM image of an individual SWNT suspended over a 3-μm-wide trench (300-nm-deep). (b) Illustration showing the Raman spectra characterization of a suspended SWNT, with the sample temperature controlled by a hot stage.

The suspended SWNTs were directly prepared by ethanol chemical vapor deposition (CVD) on trench-contained silicon substrates.[10,11] As shown in Figure 1a, individual SWNTs can be freely suspended over 3-μm-wide trenches (300 nm deep).

* Corresponding author. Address: Center for Nanoscale Science and Technology (CNST), College of Chemistry & Molecular Engineering, Peking University, Beijing 100871, P. R. China. Tel & Fax: 86-10-6275-7157. E-mail: jinzhang@pku.edu.cn.

10.1021/jp075058f CCC: $37.00

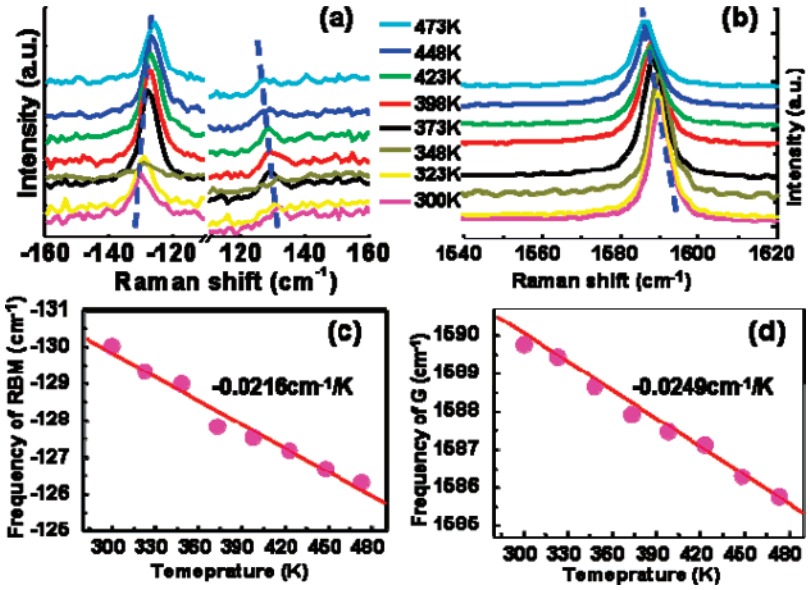

Figure 2. (a and b) Radial breathing mode (RBM) (a) and G mode (b) Raman frequency evolution with increased temperature (from bottom to top: 300, 323, 348, 373, 398, 423, 448, 473 K) of an individual SWNT. The left part in a is the anti-Stokes band. (c and d) Plot of the frequency of RBM (c) and G mode (d) vs temperature. Because the Stokes bands are relatively weak in part a, the anti-Stokes bands are used for the fitting in par c. The lines are linear fitting results for obtaining the temperature dependence of the frequency.

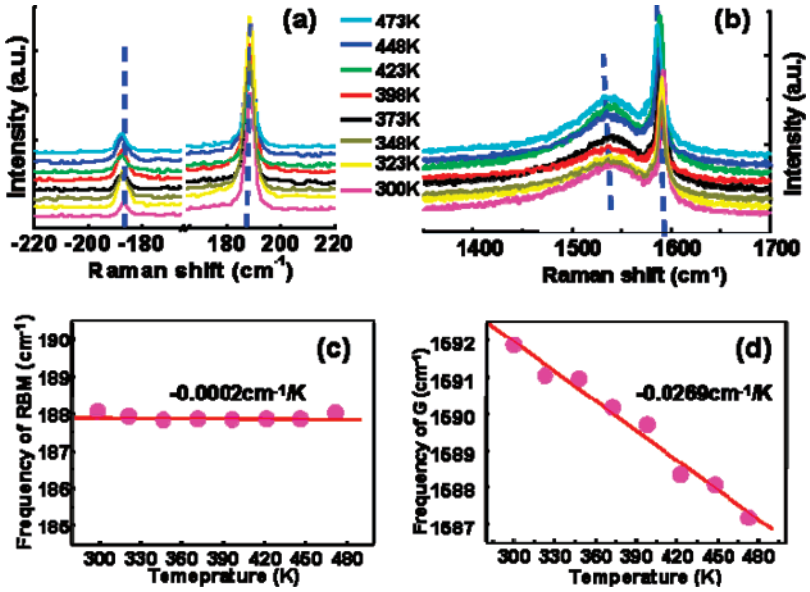

Figure 3. (a and b) Radial breathing mode (RBM) (a) and G mode (b) Raman frequency evolution with increased temperature (from bottom to top: 300, 323, 348, 373, 398, 423, 448, 473 K) of another individual SWNT, for comparison with the SWNT shown in Figure 2. (c and d) Plot of frequency of RBM (c) and G mode (d) vs temperature. The lines are linear fitting results for obtaining the temperature dependence of the frequency.

A programmable hot-stage (THMS 600) was used for heating of SWNTs, as illustrated by Figure 1b. Raman spectra of suspended SWNTs at temperature of 300, 323, 348, 373, 398, 423, 448, and 473 K were collected using micro-Raman spectroscopy. The Raman spectra wave number range was set to include the G band, and the anti-Stokes/Stokes of RBM. To ensure that the temperatures of samples were the same as the stage, we took all spectra after the temperature of the hot stage was stable for at least 10 min. The excitation energy was 1.96 eV (632.8 nm), and the spot size was 1 μm^2. The laser power used was 0.16 mW at the sample place. We have checked the laser heating effect by monitoring the intensity ratio of the anti-Stokes to the Stokes of the RBM when tuning the laser power[11,12] and no observable laser heating effect when the laser power was 0.16 mW. All of the Raman spectra were fitted by Lorentzian peak shape to obtain the peak frequency. The Raman peak of the anti-Stokes and Stokes of the RBM are symmetric, and the stronger one has been chosen for the fitting in order to get a more-precise value.

Figure 2a and b shows the RBM and G band of an individual SWNT at different temperatures. With increased temperature, ω_{RBM} and ω_G both downshift, which is consistent with previous reports.[5,14] Parts c and d of Figure 2 are plots for the relation between frequency and temperature. The temperature dependence of the frequency in terms of $d\omega/dT$ was obtained from the slope of linear fitting, which is -0.0216 cm^{-1}/K for ω_{RBM} (130 cm^{-1}) and -0.0249 cm^{-1}/K for ω_G (1590 cm^{-1}). For comparison between different SWNTs or different Raman modes, the temperature coefficient of frequency (α_ω) has been defined as $(d\omega/dT)/\omega(T = 300\ K)$.[3] For example, $\alpha_{\omega RBM}$ is $-1.66 \times 10^{-4}/K$ and $\alpha_{\omega G}$ is $-1.57 \times 10^{-5}/K$ for the results shown in Figure 2. The above value of $\alpha_{\omega G}$ is similar to what

TABLE 1: Summarized Data of Raman Frequency and Corresponding Temperature Coefficients of 13 Individual SWNTs[a]

no.	ω_{RBM} (cm^{-1})	diameter (nm)	χ_{RBM} (cm^{-1}/K)	α_{RBM} (1/K)	ω_{G+} (cm^{-1})	χ_{G+} (cm^{-1}/K)	α_{G+} (1/K)	ω_{G-} (cm^{-1})	χ_{G-} (cm^{-1}/K)	α_{G-} (1/K)
1	282.9	0.877	−0.0029	-1.03×10^{-5}	1584.5	−0.0258	-1.63×10^{-5}			
*	268 [15]			~0						
*	264 [3]			-3.41×10^{-5}						
2	*222.2*	*1.116*	*−0.0081*	-3.63×10^{-5}						
*	*197* [13]			-4.92×10^{-5}						
3	*188.0*	*1.319*	*−0.0002*	-1.06×10^{-6}	*1591.9*	*−0.0269*	-1.69×10^{-5}			
4	*186.7*	*1.328*	*−0.0100*	-5.37×10^{-5}						
*	*182* [3]			-2.48×10^{-5}						
5	*169.9*	*1.460*	*−0.0006*	-3.53×10^{-6}	*1595.6*	*−0.0207*	-1.30×10^{-5}	*1583.1*	*−0.0269*	-1.70×10^{-5}
6	156.8	1.582	−0.0063	-4.02×10^{-5}	1579.5	−0.0289	-1.83×10^{-5}			
7	151.9	1.633	−0.0192	-1.26×10^{-4}	1592.0	−0.0282	-1.77×10^{-5}	1574.2	−0.0329	-2.09×10^{-5}
8	147.9	1.677	−0.0021	-1.42×10^{-5}	1591.9	−0.0247	-1.55×10^{-5}	1584.2	−0.0243	-1.53×10^{-5}
9	146.7	1.691	−0.0184	-1.25×10^{-4}	1592.5	−0.0289	-1.81×10^{-5}			
10	141.1	1.758	−0.0017	-1.20×10^{-5}	1587.3	−0.0266	-1.68×10^{-5}	1565.8	−0.0234	-1.49×10^{-5}
11	130.0	1.908	−0.0216	-1.66×10^{-4}	1589.8	−0.0249	-1.57×10^{-5}			
12	115.3	2.151	−0.0075	-6.50×10^{-5}	1582.9	−0.0240	-1.52×10^{-5}	1579.7	−0.0314	-1.99×10^{-5}
13	113.3	2.189	−0.0261	-2.30×10^{-4}	1590.7	−0.0258	-1.62×10^{-5}			

[a] SWNTs are listed from top to bottom according their diameters from small to large. Each row corresponds to data of same SWNT. The "*" in the left column marks the data from references for comparison. According to the Kataura plot and resonance conditions, SWNT nos. 2−5 (marked with italic) are metallic and the others are semiconducting. ω_{RBM}, ω_{G+}, and ω_{G-} indicate the frequency of the corresponding Raman modes. χ_{RBM}, χ_{G+}, and χ_{G-} correspond to $d\omega_{RBM}/dT$, $d\omega_{G+}/dT$, and $d\omega_{G-}/dT$, respectively. α_{RBM}, α_{G+}, and α_{G-} are the normalized temperature coefficients of these Raman modes.

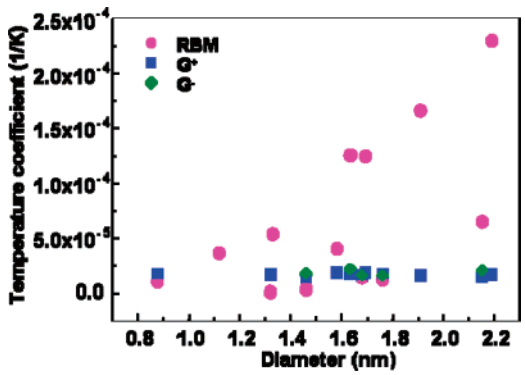

Figure 4. Plot of temperature coefficients of Raman frequency vs the diameter of nanotubes. Dots: radial breathing mode (RBM). Square: G^+ band. Triangle: G^- band. This plot shows us that the temperature coefficients of RBM have structure dependence, whereas those of the G mode do not.

has been reported for graphite[14] and bulk carbon nanotube samples.[5] But the value of $\alpha_{\omega RBM}$ is quite large compared to that reported previously, which is the following: $\alpha_{182} = -2.48 \times 10^{-5}$/K (bulk SWNT sample),[3] $\alpha_{197} = -4.92 \times 10^{-5}$/K (individual nanotube on substrate),[13] $\alpha_{264} = -3.41 \times 10^{-5}$/K (bulk SWNT sample),[3] and no change was found for $\omega_{RBM} = 268$ cm^{-1} (individual suspended nanotube, temperature range: −160 to 300 °C).[15] The results of another individual SWNT are shown in Figure 3. Its ω_{RBM} shows almost no shift with temperature increase while its ω_G downshifts, which is in contrast to Figure 2. These results suggested that the $\alpha_{\omega RBM}$ values of SWNTs may depend on their environment and peculiar structures.

To investigate the relationship between $\alpha_{\omega RBM}$ and nanotube structure, we measured the $\alpha_{\omega RBM}$ and $\alpha_{\omega G}$ values of 13 individual suspended SWNTs in the same way as described above. All of the data are summarized in Table 1, and the $\alpha_{\omega RBM}$ and $\alpha_{\omega G}$ versus nanotube diameter (d_t, $d_t = 248/\omega_{RBM}$[16]) is plotted in Figure 4. For a G band showing two obvious peaks, we analyzed them as G^+ (higher-frequency part) and G^- (lower-frequency part), respectively. As seen in Figure 4, all SWNTs show almost the same $\alpha_{\omega G}$, with a value of $(-1.67 \pm 0.20) \times 10^{-5}$/K. The $\alpha_{\omega RBM}$ values are varied from one to another, with a minimum value of -1.06×10^{-6}/K and a maximum of -2.30×10^{-4}/K. Most interestingly, the $\alpha_{\omega RBM}$ values show a diameter-dependence trend, and the $\alpha_{\omega RBM}$ values of nanotubes with similar diameters may be different.

The Raman frequency downshift with temperature is due to the softening of the C−C bond.[3] A similar $\alpha_{\omega G}$ value for different nanotubes can be readily understood considering the characteristics of the G mode. The G^+ band is associated with in-plane C−C vibrational movement along the nanotube axis, and thus, ω_{G+} is essentially independent of diameter.[1] We note that the reported $\alpha_{\omega G}$ values of both graphite and multiwalled carbon nanotubes (MWNT)[17] are about -1.7×10^{-5}/K, almost equal to our results of SWNTs $(-1.67 \pm 0.20) \times 10^{-5}$/K. Because carbon nanotubes can be envisioned as rolled-up graphene layers, the above results suggest that the convolution of graphene layer has no obvious influence on the temperature dependence of the G band.

In contrast to $\alpha_{\omega G}$, there is a remarkable difference between the $\alpha_{\omega RBM}$ values of different SWNTs, which indicates a distinct temperature effect on the RBM of different SWNTs. Because individual suspended nanotubes were used in the experiment, there was no environmental difference between these SWNTs. So the difference in $\alpha_{\omega RBM}$ should originate from the specific structures of the SWNTs. SWNTs can be envisioned as rolled-up graphene layers, and, according to the rolling vector, two parameters including diameter (d_t) and chiral angle (θ), define the structure of a SWNT.[4] RBM corresponds to vibration of carbon atoms in radial directions and consequently, ω_{RBM} is tightly dependent on diameter. Chiral angle, which defines the relative directions of C−C bonds to the RBM vibration, may also influence ω_{RBM}.

The downshift of ω_{RBM} with increased temperature can result from thermal expansion in the radial direction and softening of C−C bonds.[3,14] The $\alpha_{\omega G}$ is also related to the softening of C−C bonds and similar $\alpha_{\omega G}$ values (of both G^+ and G^-) of different SWNTs indicate that there is no remarkable difference in the extent of C−C softening. Therefore, the thermal expansion in the radial direction is supposed to be the main contribution to the difference in $\alpha_{\omega RBM}$ values. SWNTs can be envisioned as rolled-up graphene layers, and the convolution of the graphene layers will result in strain in the radial direction of the SWNTs. For SWNTs with small diameters (large curvature of the graphene layers), the strain energy due to the curvature of graphene layers is large compared to that of large-diameter

SWNTs, and that should result in smaller radial thermal expansion of small-diameter nanotubes.[3,18] Therefore, larger $\alpha_{\omega RBM}$ values are expected for nanotubes with large diameters. Additionally, as been suggested by calculational work,[4] the chiral angle and metallicity of nanotubes also influence the softening of the RBM frequency. This is consistent with the fact that even nanotubes with similar diameters, such as the two nanotubes with $\omega_{RBM} = 115.3\ cm^{-1}$($d_t \approx 2.15$ nm) and $\omega_{RBM} = 113.3\ cm^{-1}$($d_t \approx 2.19$ nm), have an obvious different $\alpha_{\omega RBM}$ values. This demonstrates the chirality dependence of $\alpha_{\omega RBM}$. However, because definite (n,m) assignments for each SWNT is difficult and there are no calculational works touching the chirality effect on $\alpha_{\omega RBM}$, we cannot get further information on this issue. One thing that needs to be mentioned here is that it is suggested[4] that the coupling of RBM to the other totally symmetric modes can also influence the softening of ω_{RBM}, and, thus, the changes in coupling may be another explanation of the difference in $\alpha_{\omega RBM}$ values.

In summary, the temperature dependence of the Raman spectra of 13 individual suspended SWNTs has been investigated and different SWNTs showed similar $\alpha_{\omega G}$ values but distinct $\alpha_{\omega RBM}$ values. The mean value of $\alpha_{\omega G}$ is -1.67×10^{-5}/K, which is similar to that of graphite and MWNTs, suggests that the tubular structure has no obvious influence on the temperature dependence of the G mode. In contrast, the $\alpha_{\omega RBM}$ values of these SWNTs are found to vary from one to another, with a minimum value of -1.06×10^{-6}/K and a maximum of -2.30×10^{-4}/K, which indicates the structure dependence of $\alpha_{\omega RBM}$. SWNTs with larger diameters tend to have larger $\alpha_{\omega RBM}$ values, and, furthermore, even SWNTs with similar diameters may show distinct $\alpha_{\omega RBM}$ values. These results reveal the diameter and chirality influence on the behaviors of RBM. These findings demonstrate the tight relationship between the properties and structures (both diameter and chiral angle) of SWNTs. Precise (n,m) assignment for individual SWNTs and calculational works may benefit further study on this issue.

Acknowledgment. This work was supported by NSFC (20573002, 20673004, 50521201), MOST (2006CB932701, 2006CB932403, 2007CB936203), and MOE (NCET-05-0008).

References and Notes

(1) Dresselhaus, M. S.; Dresselhaus, G.; Saito, R.; Jorio, A. *Phys. Rep.* **2005**, *409*, 47.

(2) Jorio, A.; Fantini, C.; Dantas, M. S. S.; Pimenta, M. A.; Souza, A. G.; Samsonidze, G. G.; Brar, V. W.; Dresselhaus, G.; Dresselhaus, M. S.; Swan, A. K.; Unlu, M. S.; Goldberg, B. B.; Saito, R. *Phys. Rev. B* **2002**, *66*, 115411.

(3) Raravikar, N. R.; Keblinski, P.; Rao, A. M.; Dresselhaus, M. S.; Schadler, L. S.; Ajayan, P. M. *Phys. Rev. B* **2002**, *66*, 235424.

(4) Kurti, J.; Zolyomi, V.; Kertesz, M.; Sun, G. *New J. Phys.* **2003**, *5*, 125.1.

(5) Li, H. D.; Yue, K. T.; Lian, Z. L.; Zhan, Y.; Zhou, L. X.; Zhang, S. L.; Shi, Z. J.; Gu, Z. N.; Liu, B. B.; Yang, R. S.; Yang, H. B.; Zou, G. T.; Zhang, Y.; Iijima, S. *Appl. Phys. Lett.* **2000**, *76*, 2053.

(6) Zhang, Q.; Yang, D. J.; Wang, S. G.; Yoon, S. F.; Ahn, J. *Smart Mater. Struct.* **2006**, *15*, S1.

(7) Fantini, C.; Jorio, A.; Souza, M.; Strano, M. S.; Dresselhaus, M. S.; Pimenta, M. A. *Phys. Rev. Lett.* **2004**, *93*, 147406.

(8) Ericson, L. M.; Pehrsson, P. E. *J. Phys. Chem. B* **2005**, *109*, 20276.

(9) Zhang, Y. Y.; Son, H. B.; Zhang, J.; Dresselhaus, M. S.; Kong, J.; Liu, Z. F. *J. Phys. Chem. C* **2007**, *111*, 1983.

(10) Zhang, Y. Y.; Zhang, J.; Son, H. B.; Kong, J.; Liu, Z. F. *J. Am. Chem. Soc.* **2005**, *127*, 17156.

(11) Zhang, Y. Y.; Son, H. B.; Zhang, J.; Kong, J.; Liu, Z. F. *J. Phys. Chem. C* **2007**, *111*, 1988.

(12) Souza, A. G.; Jorio, A.; Hafner, J. H.; Lieber, C. M.; Saito, R.; Pimenta, M. A.; Dresselhaus, G.; Dresselhaus, M. S. *Phys. Rev. B* **2001**, *63*, 241404.

(13) Zhou, Z. P.; Dou, X. Y.; Ci, L. J.; Song, L.; Liu, D. F.; Gao, Y.; Wang, J. X.; Liu, L. F.; Zhou, W. Y.; Xie, S. S.; Wan, D. Y. *J. Phys. Chem. B* **2006**, *110*, 1206.

(14) Tan, P. H.; Deng, Y. M.; Zhao, Q.; Cheng, W. C. *Appl. Phys. Lett.* **1999**, *74*, 1818.

(15) Cronin, S. B.; Yin, Y.; Walsh, A.; Capaz, R. B.; Stolyarov, A.; Tangney, P.; Cohen, M. L.; Louie, S. G.; Swan, A. K.; Unlu, M. S.; Goldberg, B. B.; Tinkham, M. *Phys. Rev. Lett.* **2006**, *96*, 127403.

(16) Jorio, A.; Saito, R.; Hafner, J. H.; Lieber, C. M.; Hunter, M.; McClure, T.; Dresselhaus, G.; Dresselhaus, M. S. *Phys. Rev. Lett.* **2001**, *86*, 1118.

(17) Huang, F. M.; Yue, K. T.; Tan, P. H.; Zhang, S. L.; Shi, Z. J.; Zhou, X. H.; Gu, Z. N. *J. Appl. Phys.* **1998**, *84*, 4022.

(18) Ci, L. J.; Zhou, Z. P.; Song, L.; Yan, X. Q.; Liu, D. F.; Yuan, H. J.; Gao, Y.; Wang, J. X.; Liu, L. F.; Zhou, W. Y.; Wang, G.; Xie, S. S. *Appl. Phys. Lett.* **2003**, *82*, 3098.